Journal of the Serbian Chemical Society
JSCS-info@shd.org.rs • www.shd.org.rs/JSCS
J. Serb. Chem. Soc. 75 (8) 1115–1124 (2010)
JSCS–4036
UDC 547.214+546.881'77–31+
544.478:66.094.258.094.3
Original scientific paper

Oxidative dehydrogenation of isobutane over supported V–Mo mixed oxides

GHEORGHIȚA MITRAN*, IOAN-CEZAR MARCU, ADRIANA URDĂ and IOAN SĂNDULESCU

Department of Technological Chemistry and Catalysis, Faculty of Chemistry, University of Bucharest, 4-12, Blv. Regina Elisabeta, 030018, Bucharest, Romania

(Received 4 December 2009)

Abstract: Vanadium–molybdenum oxides supported on Al_2O_3, CeO_2 and TiO_2 were prepared by a "wet" impregnation method, characterized using XRD, N_2 adsorption, UV–Vis spectroscopy, electrical conductivity measurements and tested in the oxidative dehydrogenation of isobutane. The catalytic performance in the oxidative dehydrogenation of isobutane at 400–550 °C depended on the nature of support and on the content of VMoO species on the support. The catalysts supported on alumina were more active and selective than those supported on ceria and titania.

Keywords: vanadia–molybdena catalysts; isobutene; oxidative dehydrogenation.

INTRODUCTION

Oxidative dehydrogenation of alkanes provides a thermodynamically accessible route to the synthesis of alkenes from alkanes.[1–9] Most catalysts for selective oxidations possess vanadium as a key element. Mixed-metal oxide catalysts are efficient for the oxidation alkanes to olefins, oxygenates and nitriles. Supported vanadium–molybdenum oxides catalyze the oxygenation of alkanes but unselective combustion pathways limit alkene selectivities.[5]

The advantages of supported metal oxides include higher mechanical strength, better thermal stability and larger surface area. However, the catalytic behavior of supported vanadium-molybdenum oxides is modified by the nature of the metal oxide support and the vanadium–molybdenum loading.

The local coordination and symmetry of Mo^{6+} and V^{5+} centers in bulk and supported catalysts have frequently been implicated in the observed effects of the support, as well as of the VO_x–MoO_x concentration and pretreatment procedures on catalytic behavior. Many of these structure–function relations remain incomp-

* Corresponding author. E-mails: mitran.gheorghita@unibuc.ro; geta_mitran@yahoo.com
doi: 10.2298/JSC091204099M

lete because of difficult structural characterization, undetected transport restrictions, and kinetic analyses, complicated by parallel and sequential combustion pathways.

The extent of dispersion and the local and extended structure of supported VO_x–MoO_x species depend on the chemical identity and the surface area of the support.[10,11] It was shown that basic metal oxides (*e.g.*, MgO and Bi_2O_3) as supports lead to supported VO_x–MoO_x species with higher alkene selectivities than when acidic oxides are used as the support.[8] Several authors have proposed that acidic VO_x–MoO_x species interact weakly with acidic supports, leading to poorly dispersed MoO_3 and V_2O_5 crystallites.

The structure of selective VO_x–MoO_x species and the reaction pathways in oxidative dehydrogenation of alkanes remain subjects of active discussion.

In this study, the effect of the support (Al_2O_3, TiO_2 and CeO_2) on the catalytic behavior of VO_x–MoO_x species in the oxidative dehydrogenation of isobutane was examined over two ranges of VO_x–MoO_x surface loadings. X-Ray diffraction, electrical conductivity measurements and UV–Visible spectroscopy were used to examine the structure and electronic properties of the catalysts.

EXPERIMENTAL

Catalysts preparation and characterization

The TiO_2 and CeO_2 supports were obtained from commercial sources. Al_2O_3 was prepared from $Al(NO_3)_3{\cdot}9H_2O$ by co-precipitation at a controlled pH. V_2O_5–MoO_3 was introduced at two concentration levels, 5 % and 10 %, *via* incipient wet impregnation of the supports with aqueous NH_4VO_3 and $(NH_4)_6MoO_{24}{\cdot}4H_2O$ solutions. The ratio between the V-containing and Mo-containing reactants was set so that the supported component had the composition 10 % V_2O_5–90 % MoO_3. After impregnation, the samples were dried in air at 100 °C and then calcined at 600 °C for 4 h.

Powder X-ray diffraction (XRD) patterns were obtained using a Bruker D5005 diffractometer and CuKα radiation. They were recorded with 0.02° (2θ) steps over 3–70° angular range with a 1s counting time per step.

The surface areas of the catalysts were measured from N_2 adsorption isotherms at 77 K by the BET method using an ASAP 2000 sorptometer.

Diffuse reflectance UV–Visible spectra were obtained using MgO as the reference on a Varian-Cary 4 spectrophotometer equipped with a Harrick diffuse-reflectance attachment. The reflectance data were converted to absorption spectra using Kubelka–Munk functions. The sample cell was equipped with a heater unit, a water-cooling system, a thermocouple and a gas flow system for *in situ* measurements.

The electrical conductivity of the different samples was investigated using a cell specially designed to study the electronic interactions between the samples and various gaseous atmospheres. A pastille of catalyst was placed between two platinum electrodes. The temperature of each electrode was given by a thermocouple the wires of which were also used as connections for the electrical measurements. Hence, semi-quantitative comparisons between solids could be made and the electrical conductivity measurements provided an estimate of the variations in the concentration of the main charge carriers as a function of physical para-

meters, such as temperature and the nature of the gas, under conditions as close as possible to those of the catalytic reaction.

Catalytic activity tests

The oxidative dehydrogenation of isobutane was realized in a fixed bed quartz tube down-flow reactor (i. d. 15 mm) operated at atmospheric pressure. Quartz chips were placed above and below the catalyst bed to reduce the reactor void volume and to avoid homogeneous reactions in the free space. The temperature of the catalyst bed was monitored by a thermocouple in a coaxial thermo-well in its center. The gas mixture consisting of isobutane and air was fed into the reactor at a volume hourly space velocity (*VHSV*) in the range of 1000–2500 h^{-1}. The reaction temperature was varied between 400 and 550 °C, the isobutane/O_2 molar ratio, between 0.5 and 2, while the catalyst bed volume was always kept to 2 cm^3.

In all studies, the reactor effluent was passed through a condenser to remove water and liquid oxygenated products. Gas-phase reactants and products were analyzed with a Thermo Finnigan gas chromatograph equipped with a flame ionization detector and a thermal conductivity detector. Chromatograph separation was accomplished with an alumina column and a CTRI column. The condensate was analyzed with a Thermo Finnigan chromatograph using a DB-5 column and a flame ionization detector. Isobutene, CO and CO_2 were the major products formed under the employed reaction conditions. Minor amounts of the liquid oxygenated products, acetic acid, methacrolein and unknowns, were detected. Conversion of isobutane and olefin selectivity is expressed as mol % on a carbon atom basis. The carbon balance was in all runs greater than 95 %.

RESULTS AND DISCUSSION

Catalysts characterization

The surface areas of the catalysts are given in Table I. The surface areas of the catalysts supported on Al_2O_3 were much higher than those of the catalysts supported on CeO_2 and TiO_2. It can also be observed that an increase of the support coverage led to a sharp drop in the surface area for the alumina-supported vanadia–molibdena catalysts. This was not the case for the ceria- and titania-supported catalysts.

TABLE I. V_2O_5–MoO_3 content, surface area and activation energy of conduction in air for the studied supported vanadium-molybdenum oxide catalysts

Support	Catalyst	V_2O_5–MoO_3 content mass %	BET Surface area m^2/g	Activation energy of conduction in air kJ mol^{-1}
Al_2O_3	5VMoO/Al_2O_3	5	298	–
	10VMoO/Al_2O_3	10	195	–
TiO_2	5VMoO/TiO_2	5	5.6	88.5
	10VMoO/TiO_2	10	6.5	73.3
CeO_2	5VMoO/CeO_2	5	3.3	62.8
	10VMoO/CeO_2	10	3.4	53.4

The X-ray diffraction measurements (Fig. 1) showed that the MoO_x–VO_x species were dispersed on the support but that they did not influence the

crystallinity of the rutile TiO_2 and ceria CeO_2 structure. Bulk V_2O_5 and MoO_3 crystallites were not detected at any MoO_x–VO_x loading on alumina and also not on titania- and ceria-supported samples with the lower MoO_x–VO_x loading. The higher loading on TiO_2 led to the appearance of orthorhombic Mo_4O_{11} crystallites and on Al_2O_3 led to the appearance of triclinic aluminum vanadium oxide – $AlVO_4$, tetragonal vanadyl molybdenum oxide – $VOMoO_4$, and monoclinic molybdenum vanadium oxide – $Mo_{0.67}V_{0.33}O_2$.

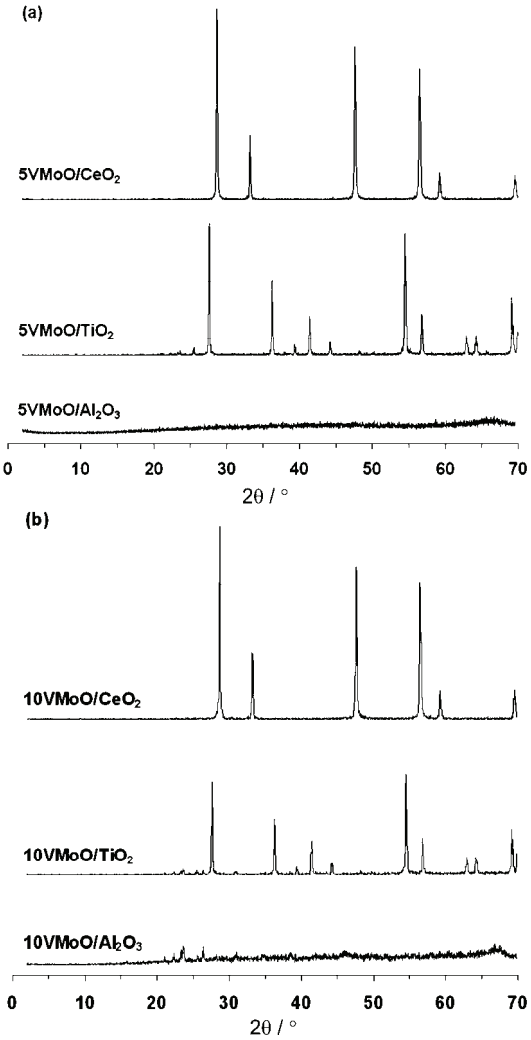

Fig. 1. X-Ray diffraction patterns for $VMoO/Al_2O_3$, $VMoO/TiO_2$ and $VMoO/CeO_2$; a) 5VMoO/support, b) 10VMoO/support.

The UV–Vis spectra of the catalysts are comparatively shown in Fig. 2. The absorption bands detected in the range 250–450 nm are mainly related to the presence of Mo^{6+} and V^{5+} in an octahedral environment.[12,13] The band observed at

340 nm is attributed to Mo6+ in octahedral coordination with tetragonal distortion. The spectrum shows a band at 350–400 nm, typical of charge transfer of V^{5+} species in octahedral symmetry.[14,15] This band, which is large and asymmetric, can be interpreted by charge transfer of O^{2-} to V^{5+} in the V=O bond or by the presence of polymeric chains of distorted VO_6 as a monolayer on the support. The 320–330 nm bands indicate a local interaction between molybdenum and vanadium. This is evidence for the high mobility of these species at the surface of the support.

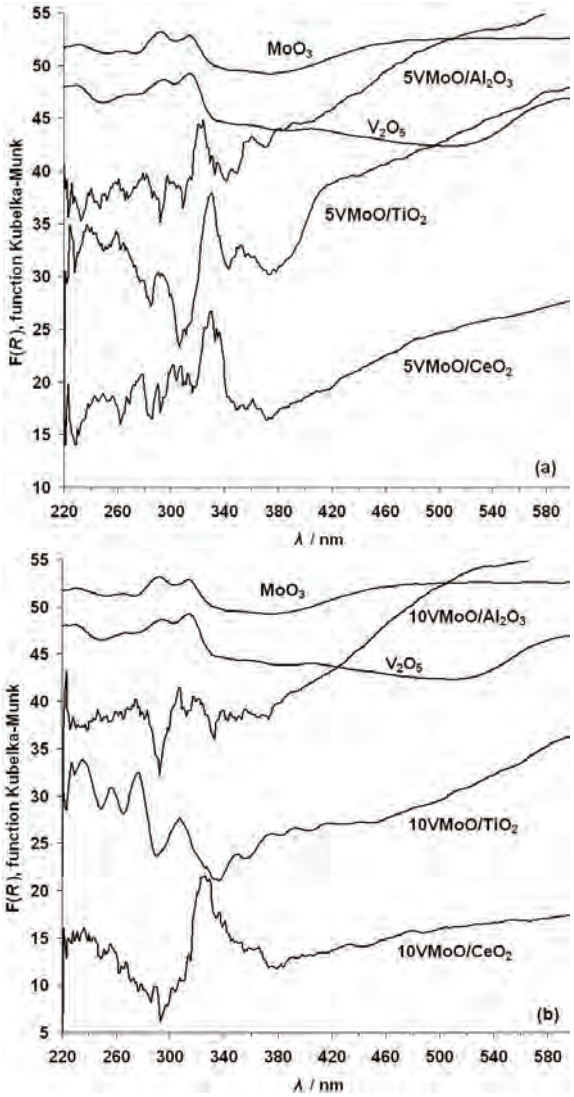

Fig. 2. UV–Visible spectra of the supported V–Mo–O catalysts;
a) 5VMoO/support,
b) 10VMoO/support.

The electrical conductivities of the titania and ceria-supported catalysts were measured as a function of temperature under air, nitrogen and isobutane at atmospheric pressure. Applying the Heckelsberg criterion,[16] the nature of the semiconductor type of a solid can be determined. To ensure the reversibility of the experiments, the measurements were performed with increasing and decreasing temperature. The obtained semi-log plots (log $\sigma = f(1/T)$) are given in Fig. 3.

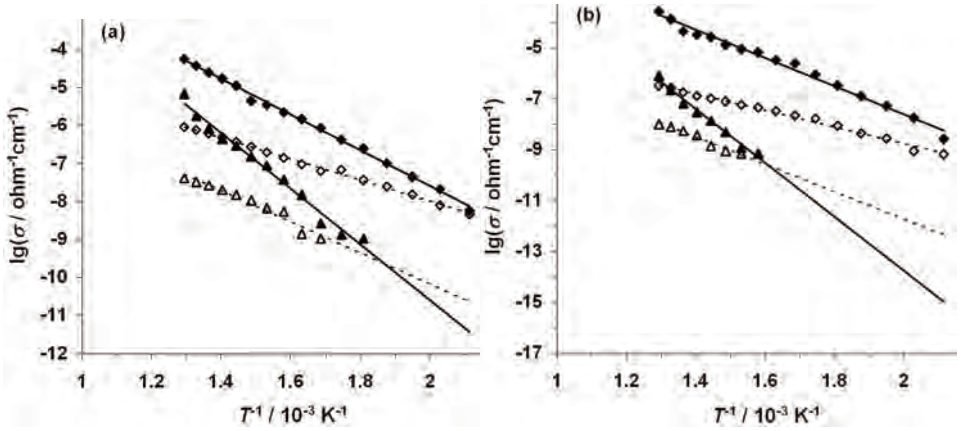

Fig. 3. Arrhenius plots of the electrical conductivity for the a) 5VMoO/support and b) 10VMoO/support catalyst; air (◊, Δ) and isobutane (♦,▲) ♦ – CeO_2, ▲ – TiO_2.

Variations in conductivity for mixed or for supported oxides are generally attributed to a doping effect.[17] This phenomenon results from the dissolution of heterovalent ions in the lattice of the host oxide, which creates free charge carriers (electrons or holes) according to the valence induction law. This dissolution is favored by calcination at high temperature of the support impregnated with the precursor of the deposited oxide. For *n*-type semiconductors, such as TiO_2 and CeO_2, an increase in σ results from the dissolution of a heterocation with a valence higher than 4. The deposition of MoO_x–VO_x species by impregnation and calcination is probably accompanied by a partial dissolution of V^{5+} and Mo^{6+} in the surface sub-layers of TiO_2 and CeO_2. The substitution of a Ti^{4+} by a V^{5+} or a Mo^{6+} induces free conduction electrons. If pentavalent V^{5+} or hexavalent Mo^{6+} are inserted into tetravalent sites, they can only share four valence electrons with four neighboring O^{2-}. The fifth and the sixth electron cannot be shared and are delocalized around the V^{5+} and the Mo^{6+} positive centers. Only a small amount of thermal energy is required for the delocalization of these electrons and their promotion into the conduction band.

For catalysts supported on CeO_2, the electrical conductivity is higher than for catalysts supported on TiO_2. As expected, the electrical conductivity of the catalytic materials increased with increasing amount of deposited VO_x–MoO_x. Since these materials are predominantly *n*-type semiconductors, the dependence

of the conductivity on the VO_x–MoO_x loading is attributed to an increase in the concentration of free electrons in the conduction band. On replacing air by isobutane, the total conductivity of the supported VO_x–MoO_x material increased. When the VO_x–MoO_x/TiO_2 and VO_x–MoO_x/CeO_2 materials were exposed to a reducing atmosphere, the electrical conductivity increased by several orders of magnitude, due to the reduction of the catalytic material and the formation of anion vacancies with two electrons (Eq. 1). These electrons can be readily promoted into the conduction band:

$$(O^{2-})^0 + \text{i-}C_4H_{10} \rightarrow \text{i-}C_4H_8 + H_2O + (V_O)^0 \quad (1)$$

where $(O^{2-})^0$ represents an oxygen anion of the solid. The zero-charge superscript indicates that it is a neutral entity with respect to the solid. $(V_O)^0$ represents a filled anionic vacancy with the two electrons of the former anion trapped.

Catalytic testing

The catalytic data obtained in the oxidative dehydrogenation of isobutane are presented in Table II. It can be observed that the alumina-supported catalysts were the most active, followed by the ceria- and titania-supported ones. Simultaneously, the isobutene selectivity decreased in the same order: V–Mo/Al_2O_3 > > V–Mo/CeO_2 > V–Mo/TiO_2. One likely advantage of using high surface area alumina is the possibility of a better dispersion of the active sites on the surface of the support. On the other hand, it seems that the acidic character of alumina did not negatively influence the catalytic behavior of the catalysts. The catalytic activity increased with increasing vanadia–molibdena loading for all supports, which was accompanied by a decrease of the isobutene selectivity. It should be emphasized that the catalytic activities of the supported oxides were higher than that of the respective unsupported oxide.[18]

In agreement with the redox mechanism of the oxidative dehydrogenation, a higher concentration of free electrons implies a higher rate of incorporation of gas-phase oxygen into lattice oxygen (the active oxygen species, which influences the rate of isobutane activation).

It should be noted that, for ceria- and titania-supported catalysts, the catalytic performances were better for the solids with a higher conductivity. 5VMoO/TiO_2 that exhibited the poorest catalytic properties is also the least conductive solid. Its activation energy of conduction (Table I), which is directly connected to the heat of formation of anionic vacancies, is the highest. This indicates that the endothermic reduction of 5VMoO/TiO_2 requires more energy.

The conversion of isobutane and the selectivity to isobutene for the supported MoO_x–VO_x catalysts as a function of the reaction temperature are shown in Fig. 4. The conversion of isobutane increased with increasing reaction temperature for all catalysts. The selectivity to isobutene passed through a maximum at temperatures between 450 and 500 °C.

In the UV–Vis spectra, the band corresponding to the Mo–V interaction (330 nm) had the smallest intensity for the 10VMoO/Al_2O_3 catalyst compared to the other supports. It can be also observed that the intensity of these bands decreased with increasing amount of active component. It is considered that the interaction between Mo and V is responsible for the catalytic activity since a correlation was observed between the intensity of these bands and the activity of the catalyst.

TABLE II. Catalytic performance of the supported vanadium–molybdenum oxide catalysts in the oxidative dehydrogenation of isobutane (*VHSV* = 1500 h^{-1}, molar ratio isobutane to O_2: 2:1)

Catalyst	*t* / °C	Conversion, %	Selectivity, %		
			i-C_4H_8	Cracking products	CO_x
5VMoO/Al_2O_3	450	15.0	73.5	8.5	18.0
	500	22.2	72.3	9.4	18.3
5VMoO/CeO_2	450	12.9	58.3	8.1	33.6
	500	17.3	59.9	9.8	20.3
5VMoO/TiO_2	450	10.7	48.0	4.2	47.8
	500	16.8	50.7	8.8	40.5
10VMoO/Al_2O_3	450	20.0	69.0	8.4	25.1
	500	25.5	70.5	7.8	19.2
10VMoO/CeO_2	450	15.2	53.7	7.6	38.7
	500	20.7	55.0	8.1	24.8
10VMoO/TiO_2	450	12.3	44.0	7.1	48,9
	500	18.5	48.1	11.3	40.6

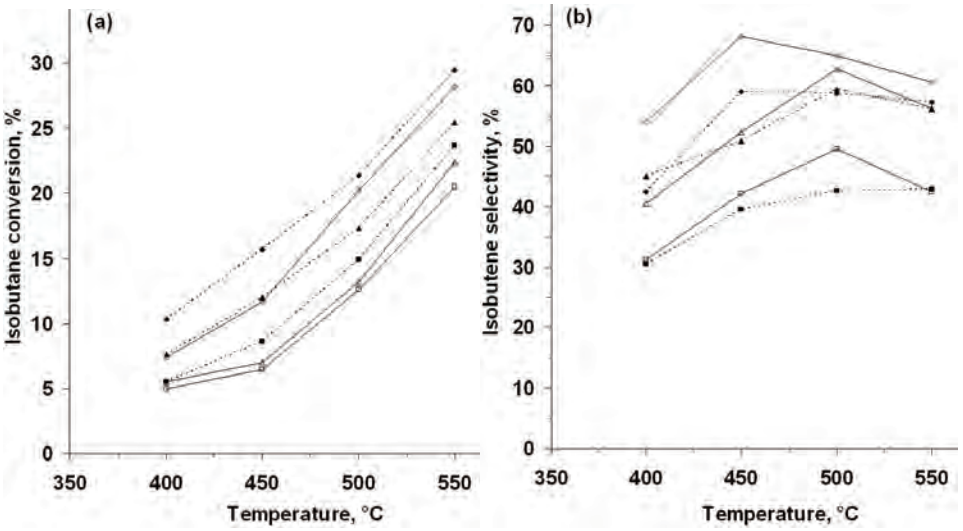

Fig. 4. Variation of the isobutane conversion (a) and isobutene selectivity (b) with the reaction temperature over supported V–Mo–O catalysts (*VHSV* = 2000 h^{-1}, *i*-C_4H_{10}:O_2 molar ratio: 1); ♦ – VMoO/Al_2O_3, ■ – VMoO/TiO_2, ▲ – VMoO/CeO_2 (—, 5 %; ····,10 %).

CONCLUSIONS

Promising catalytic results were obtained for the dehydrogenation of isobutane in presence of oxygen using Mo–V–O/supported catalysts. The use of alumina as the support with a high surface area led to an increase of both the catalytic activity and the selectivity to isobutene.

The electrical conductivity measurements clearly indicated that the ceria- and titania-supported systems are *n*-type semiconductors, and it was shown that the catalytic performances were better on catalysts with a higher conductivity.

Increasing the amount of active component led to a higher catalytic activity, but a diminished selectivity to isobutene.

ИЗВОД

ОКСИДАЦИОНА ДЕХИДРОГЕНИЗАЦИЈА ИЗОБУТАНА ПРЕКО V–Mo МЕШОВИТИХ ОКСИДА НАНЕТИХ НА ПОДЛОГУ

GHEORGHIŢA MITRAN, IOAN-CEZAR MARCU, ADRIANA URDĂ и IOAN SĂNDULESCU

Department of Technological Chemistry and Catalysis, Faculty of Chemistry, University of Bucharest, 4-12, Blv. Regina Elisabeta, 030018, Bucharest, Romania

Ванадијум–молибден оксиди нанети на подлоге од Al_2O_3, CeO_2 и TiO_2 мокрим поступком карактерисани су применом рентгенске дифракционе анализе, адсорпцијом азота, UV–Vis спектроскопијом, мерењем електричне проводљивости и тестирањем активности у реакцији оксидативне дехидрогенизације изобутана. Каталитичке особине особине оксидативне дехидрогенизације изобутана у температурном интервалу 400–550 °C зависе од природе носача и садржаја VMoO врста на носачу. Катализатори нанети на алуминијум-оксид су много активнији од катализатора који су нанети на титаноксид или церијум-оксид.

(Примљено 4. децембра 2009)

REFERENCES

1. P. Botella, J. M. López Nieto, B. Solsona, A. Mifsud, F. Márquez, *J. Catal.* **209** (2002) 445
2. P. Botella, J. M. López Nieto, A. Dejos, M. I. Vásquez, A. Martínez-Arias, *Catal. Today* **78** (2003) 507
3. H. Jiang, W. Lu, H. Wan, *J. Mol. Catal. A* **208** (2004) 213
4. K. Oshihara, T. Hisano, W. Ueda, *Top. Catal.* **15** (2001) 153
5. M. Banares, S. Khatib, *Catal. Today* **96** (2004) 251
6. Y. Takita, X. Qing, A. Takami, H. Nishiguchi, K. Nagaoka, *Appl. Catal. A* **296** (2005) 63
7. S. N. Koc, G. Gurdag, S. Geissler, M. Guraya, M. Orbay, M. Muhler, *J. Mol. Catal.* **225** (2005) 197
8. B. Solsona, A. Dejoz, T. Garcia, P. Concepción, J. M. Lopez Nieto, M. I. Vázquez, M. T. Navarro, *Catal. Today* **117** (2006) 228
9. T. V. Malleswara Rao, E. Vico-Ruiz, M. A. Bańares, G. Deoa, *J. Catal.* **258** (2008) 324
10. S. Albonetti, F. Cavani, F. Trifiro, *Catal. Rev. Sci. Eng.* **38** (1996) 413
11. G. Centi, *Appl. Catal. A* **147** (1996) 267
12. H. Aritani, T. Tanaka, T. Funabiki, S. Yoshida, K. Eda, N. Sotani, M. Kudo, S. Hasegawa, *J. Phys. Chem.* **100** (1996) 19495

13. E. García-Gonzáles, J. M. López Nieto, P. Botella, J. M. González-Calbet, *Chem. Mater*. **14** (2002) 4416
14. G. Centi, S. Perathoner, F. Trifirò,, A. Aboukais, C. F. Aisi, M. Guelton, *J. Phys. Chem*. **96** (1992) 2617
15. M. Scraml-Marth, A. Wokaun, A. Baiker, *J. Catal*. **124** (1990) 86
16. L. F. Heckelsberg, A. Clark, G. C. Bailey, *J. Phys. Chem*. **60** (1956) 559
17. J. M. Herrmann, J. Disdier, G. Deo, I. Wachs, *J. Chem. Soc. Faraday Trans*. **93** (1997) 1655
18. G. Mitran, I. C. Marcu, A. Urda, I. Sandulescu, *Revue Roumaine de Chimie* **53** (2008) 383.